

Numerical study of the pullout behavior of twisted steel fiber-reinforced concrete

Giulia T. Caravello¹, Marcello Congro^{1,2}, Deane Roehl^{1,2}

¹*Department of Civil and Environmental Engineering, Pontifical Catholic University of Rio de Janeiro, PUC-Rio, Brazil.*

²*Multiphysics Modeling and Simulation Group, Tecgraf Institute, Pontifical Catholic University of Rio de Janeiro, PUC-Rio, Brazil.*

Rua Marquês de São Vicente, 225, Gávea, Rio de Janeiro, Brazil

giuliatcaravello@tecgraf.puc-rio.br, marcellocongro@tecgraf.puc-rio.br, deane@tecgraf.puc-rio.br

Abstract. In recent years, fiber-reinforced concrete has significantly increased in civil construction due to its excellent mechanical properties. However, an in-depth study of the fiber/matrix interaction is crucial to understand the interface mechanisms between these materials. This investigation of the interface is also necessary to accurately select the mathematical formulation for simulating the mechanical behavior of twisted fibers in finite element (FE) models. This paper introduces an elastoplastic finite element model to simulate the pullout behavior of twisted steel fiber-reinforced concrete. A surface-to-surface interaction with cohesive interface elements and an exponential damage law is employed to simulate the debonding of the fiber at the interface. Sensitivity analyses are conducted to determine which contact parameters influence the pullout response, given that many calibrated variables lack a physical interpretation. Subsequently, the numerical results are validated against the experimental data obtained from laboratory pullout tests. The results demonstrate a good correlation with experimental references, confirming that the FE elastoplastic model with contact accurately predicts the pullout behavior of the composite material.

Keywords: pull-out, twisted steel fibers, cementitious composite materials, damage mechanisms, finite element analysis.

1 Introduction

In recent years, fiber-reinforced cementitious composite materials have gained prominence in the construction industry due to their excellent mechanical properties, driven by the pursuit of more efficient and durable structural solutions. The incorporation of fibers into the cementitious matrix has been extensively investigated to enhance ductility, control crack propagation, and improve energy absorption capacity [1]. Steel fiber reinforcement in cementitious matrices has various practical applications, including pavements, tunnel repairs, airport runways, and precast elements [2]. This popularity is due to the versatility of fibers, which can be manufactured in a variety of sizes and shapes, optimizing adhesion between the fiber and the cementitious matrix.

Recently, twisted fibers have been proposed to increase the bond strength with the concrete matrix by enhancing resistance to pullout and the energy dissipated due to the increasing pressure applied to the cementitious matrix along their length during uncoiling [3]. The increase in the lateral surface area in increased friction and adhesion forces for the same cross-sectional area, contributing to greater pullout resistance. To better understand the material's performance, it is essential to study the mechanism of a single twisted fiber being pulled out from the matrix.

The efficiency of crack control using twisted fibers has been demonstrated in various studies due to their

strong adhesion to the matrix and high pullout resistance by friction. The mechanical properties of cementitious composite materials reinforced with twisted fibers heavily depend on the interaction mechanism between the fiber and the matrix [4]. According to Congro [5], fibers transfer stresses from cracks to the concrete matrix, preventing crack propagation and aiding crack control.

Initially, the twisted fiber is fully bonded to the cementitious matrix, with shear stress at the fiber-matrix interface. Unlike other geometries of steel fibers, the twisted fiber undergoes an untwisting process during pullout: as the load increases, the stress at the fiber-matrix interface reaches a critical level, initiating the untwisting of the fiber. This mechanism occurs due to the helical shape of the fiber, which begins to unwind under the applied load. As untwisting progresses, the fiber starts to slide out of the matrix while still being resisted by friction and mechanical interlocking. Matrix spalling is also observed during this process, as indicated in Fig. 1. The untwisting process requires additional energy, thereby increasing the resistance to pullout. Eventually, as the applied load continues to increase, the untwisting and debonding propagate along the entire length of the fiber, resulting in complete pullout. The fiber is fully extracted from the matrix, and the load drops sharply once the fiber is entirely removed [6].

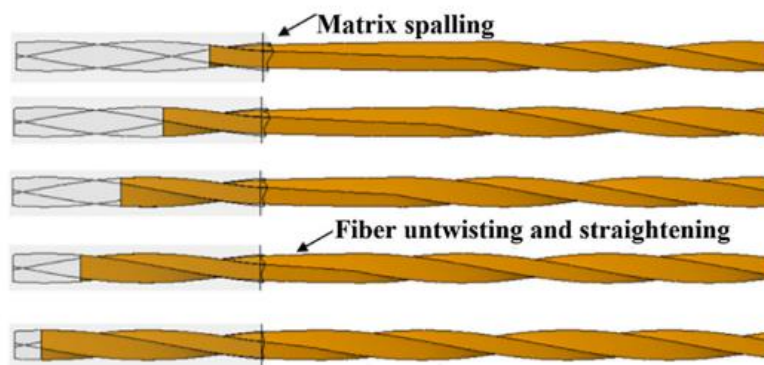


Figure 1. Mechanisms associated with the pullout of twisted steel fibers [7].

Despite the available experimental studies and numerical models, mathematical formulations that focus on the mechanisms of damage mapping and stress transfer interactions at the cement interface, particularly with twisted fiber geometries, have not yet been developed. Therefore, the main objective of this paper is to enhance the understanding of damage mechanisms in cementitious materials reinforced with twisted steel fibers. To achieve this goal, this work proposes an elastoplastic finite element model to simulate the pullout behavior of twisted steel fiber-reinforced concrete, developed based on experimental pullout tests. The numerical model allows for the identification of plastic strain concentrations captured during the analysis, corresponding to the detected damage. This highlights a greater concentration along the length of the twisted steel fiber, as well as at the fiber exit point.

2 Methodology

2.1 Concrete damaged plasticity constitutive model

The concrete damage plasticity (CDP) model has been originally developed by Rabotnov [8], where the material constitutive equation with scalar isotropic damage can be expressed according to Equation 1.

$$\sigma = (1 - d) D_0^{el} : (\varepsilon - \varepsilon^{pl}) \quad (1)$$

where σ is the Cauchy stress tensor, d is the scalar stiffness degradation variable, ε is the strain tensor and D_0^{el} is the initial/undamaged elastic material stiffness. The effective stress tensor can be defined according to Equation 2.

$$\bar{\sigma} = D_0^{el} : (\varepsilon - \varepsilon^{pl}) \quad (2)$$

where ε^{pl} is the plastic strain. The evolution of the damage scalar variable is governed by a set of the effective stress tensor $\bar{\sigma}$ and hardening/softening variables $\bar{\varepsilon}^{pl}$. The stiffness degradation is initially isotropic and defined by degradation variable d_c in a compression zone and variable d_t in a tension zone. Finally, the Cauchy stress tensor is related to the effective stress tensor $\bar{\sigma}$ through the scalar degradation parameter $(1 - d)$, as expressed in Equation 3.

$$\sigma = (1 - d) \bar{\sigma} \quad (3)$$

The damage states in tension and compression are defined independently by two hardening variables $(\bar{\varepsilon}_t^{pl}, \bar{\varepsilon}_c^{pl})$, which are referred to equivalent plastic strains in tension and compression, respectively (Equation 4). The evolution of the hardening variables is given by Equation 5.

$$\bar{\varepsilon}^{pl} = \begin{bmatrix} \bar{\varepsilon}_c^{pl} \\ \bar{\varepsilon}_t^{pl} \end{bmatrix} \quad (4)$$

$$\dot{\bar{\varepsilon}}^{pl} = h(\bar{\sigma}, \bar{\varepsilon}^{pl}) \cdot \dot{\varepsilon}^{pl} \quad (5)$$

The plastic flow is governed by a flow potential function $G(\bar{\sigma})$ defined in the effective stress space according to the non-associative flow rule given by Equation 6.

$$\dot{\varepsilon}^{pl} = \dot{\lambda} \frac{\partial G(\bar{\sigma})}{\partial \bar{\sigma}} \quad (6)$$

For the CDP model, four constitutive parameters identify the shape of the flow potential surface and the yield surface. In this model, for the flow potential G , the Drucker-Prager hyperbolic function is considered, as presented in Equation 7.

$$G = \sqrt{(f_c - m f_t t g \beta)^2 + \bar{q}^2} - \bar{p} t g \beta - \sigma \quad (7)$$

where f_t and f_c are the uniaxial tensile and compressive strengths of concrete, respectively. Moreover, β is the dilation angle measured in the p - q plane at high confining pressure, while m is an eccentricity of the plastic potential surface. The flow potential surface is defined in the p - q plane, where $\bar{p} = -\frac{1}{3}\bar{\sigma}I$, I is the effective hydrostatic stress and $\bar{q} = \sqrt{\frac{3}{2}\bar{S} \cdot \bar{S}}$ is the Mises equivalent stress. In addition, \bar{S} is the deviatoric part of the effective stress tensor $\bar{\sigma}$.

The non-associative flow rule requires a loading surface definition. The plastic damage concrete model uses a yield condition based on the loading function described in Equation 8 and proposed by Lubliner *et al.* [9].

$$F = \frac{1}{1-\alpha} (\bar{q} - 3 \alpha \bar{p} + \theta(\bar{\varepsilon}^{pl}) \langle \bar{\sigma}_{max} \rangle - \gamma \langle -\bar{\sigma}_{max} \rangle) - \bar{\sigma}_c(\bar{\varepsilon}_c^{pl}) \quad (8)$$

Other parameters, such as the tensile uniaxial strength and the uniaxial or biaxial compressive strength of concrete should be taken from experimental curves.

2.2 Numerical model

A 2D plane stress finite element model carried out to analyze a twisted steel fiber pullout test. The elastoplastic CDP model is adopted for the cement matrix, while a perfect plastic behavior is considered for the steel fiber. The simulations were carried out in the commercial software ABAQUS®. Figure 2 presents the schematic geometric representation and the boundary conditions for the twisted fiber pullout numerical model, where a prescribed displacement δ is applied at the fiber top node.

The numerical parameters that describe the constitutive models for the cement matrix and the fiber depend on these materials' stress-strain curves in tension and compression. The nonlinear behavior of the matrix/fiber interface is given by a surface-to-surface contact formulation. Two contact surfaces are established: the leader surface, referring to the matrix, and a follower surface, associated with the longitudinal fiber length. A traction-separation zone associated with a damage constitutive model with exponential law evolution is considered along the entire embedded lateral length of the fiber. Additionally, a tangential behavior is considered for the interface

between the fibers' horizontal base and the matrix through the definition of a friction coefficient, calibrated considering the experimental load-displacement curve of the test.

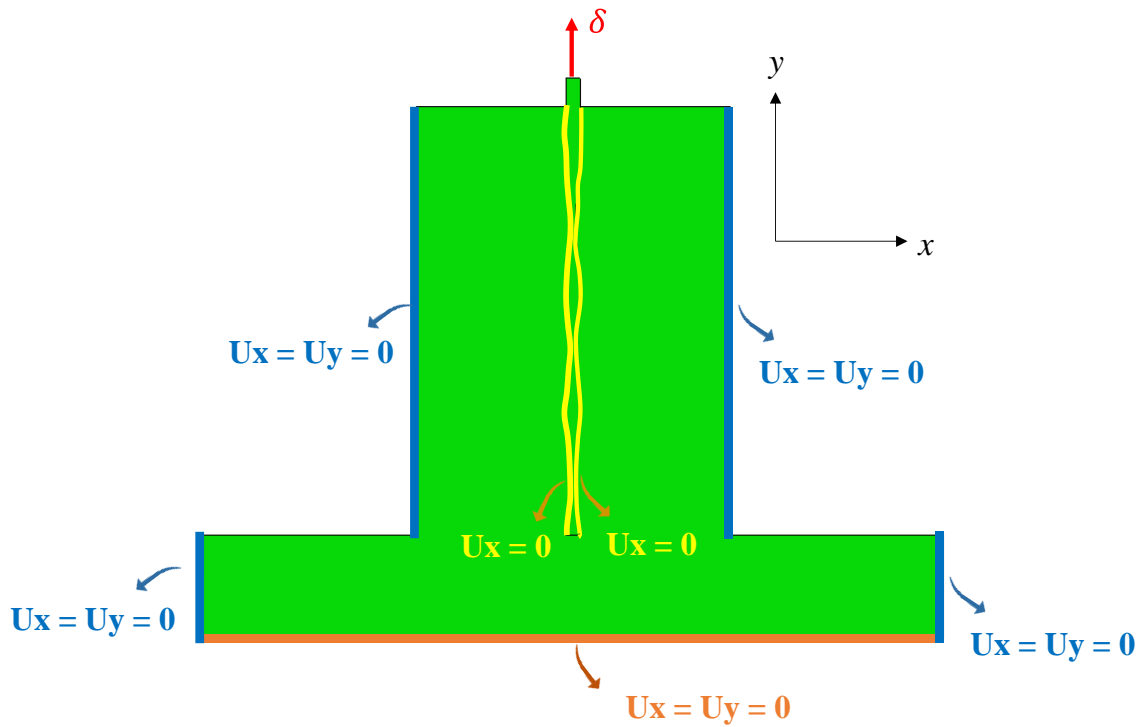


Figure 2. Model geometry and boundary conditions (U refers to displacement variable).

This case study considers an experimental test developed at Laboratório de Estruturas e Materiais (LEM/DEC) of PUC-Rio. The geometry of the model was configured in 2D, based on the test specimens molded for the experimental tests. Due to symmetry, half of the specimen was simulated. Figure 3 presents the defined geometries for the cementitious matrix and the twisted fiber positioned in the sample. The complete model presents 5136 quadratic quadrilateral elements (CPS8) with a full integration scheme, as indicated in Fig. 4.

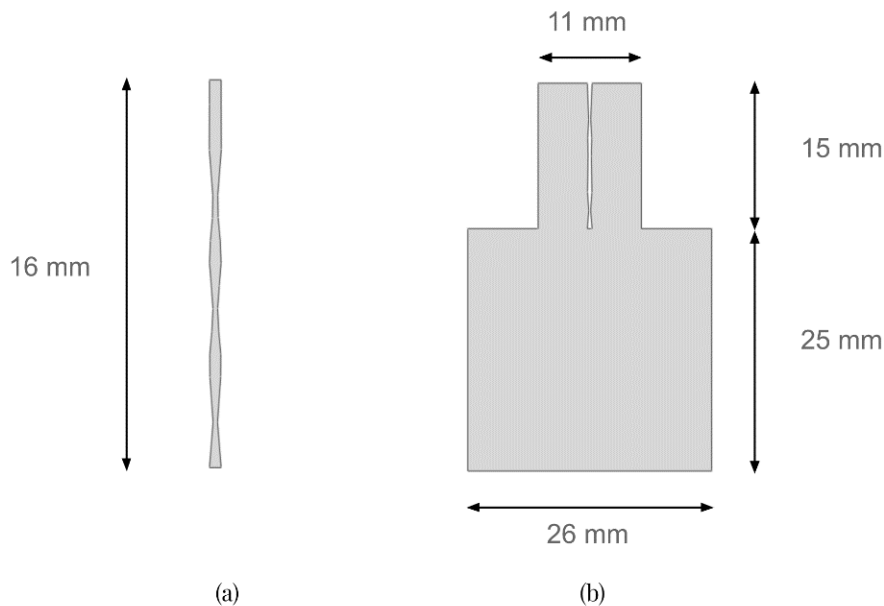


Figure 3. Geometry and dimensions of the parts: (a) twisted fiber; (b) cement matrix.

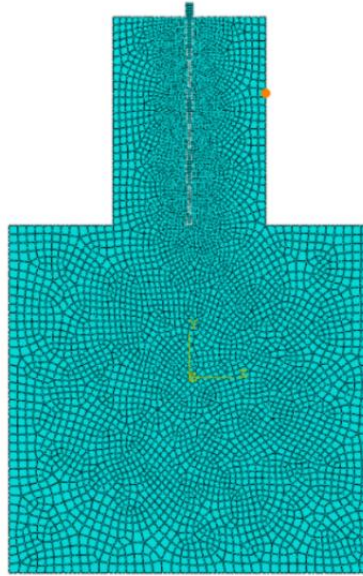


Figure 4. Mesh with 5136 elements of the model.

The elastic parameters of the cement matrix and the mechanical parameters necessary for the CDP model, using typical values for cement as established by previous studies in the literature [10], [11] are detailed in Tab. 1. The steel fiber was modeled adopting a perfectly plastic behavior with a Young's modulus of 200 GPa, a Poisson's ratio of 0.3, and a tensile strength of 1225 MPa.

Table 1. Elastic and mechanical parameters for the cement matrix.

Parameter	Value
Young's modulus (GPa)	29.60
Poisson ratio (-)	0.25
Tensile strength (MPa)	4.79
Compressive strength (MPa)	42.65
Dilation angle (°)	38.00
Eccentricity (-)	0.10
f_{b0}/f_{c0} (-)	1.16
K (-)	0.67
Viscosity parameter	0.00

The numerical pullout model presented in this paper does not consider matrix shrinkage. However, it does incorporate the nonlinear geometric effects resulting from large fiber deformations in the simulations. This model enables the determination of the pullout load-displacement behavior and facilitates the analysis of all stress transfer mechanisms during the test, with particular focus on the fiber/matrix interface region. The interface properties are calibrated based on the pullout experimental curve, adjusting parameters such as the friction coefficient and damage variables through a trial-and-error method. The final parameters are listed in Tab. 2. Details regarding the experimental setup and test will be published in a future article.

Table 2. Interface parameters for the matrix and twisted steel fiber after calibration with experimental results.

Parameter	Value
Friction coefficient μ (-)	0.2
Damage initiation δ_i (mm)	0.9
Cohesive stiffness K (MPa/mm)	8.5
Exponential damage parameter α (-)	1.0

3 Results and Discussion

The model is simulated in the commercial software ABAQUS®, and the results are compared with the corresponding experimental curves. Considering the parameters defined for the development of the numerical model, such as those for the twisted steel fiber, the cementitious matrix, the model geometry, and the calibrated parameters for defining the fiber-matrix interaction, it was possible to obtain the load-displacement response for the pullout of the twisted steel fiber from the cementitious matrix model, as shown in Fig. 5. The numerical model allows for the identification of plastic zones captured during the analysis, corresponding to the detected damage. This highlights a greater concentration along the length of the twisted steel fiber, as well as at its end (Figure 6).

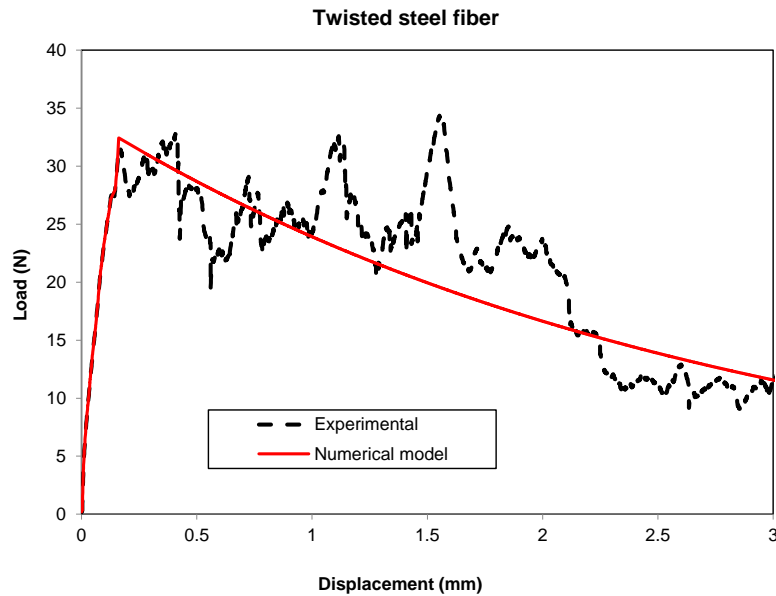


Figure 5. Load-displacement behavior of twisted steel fiber pullout in matrix.

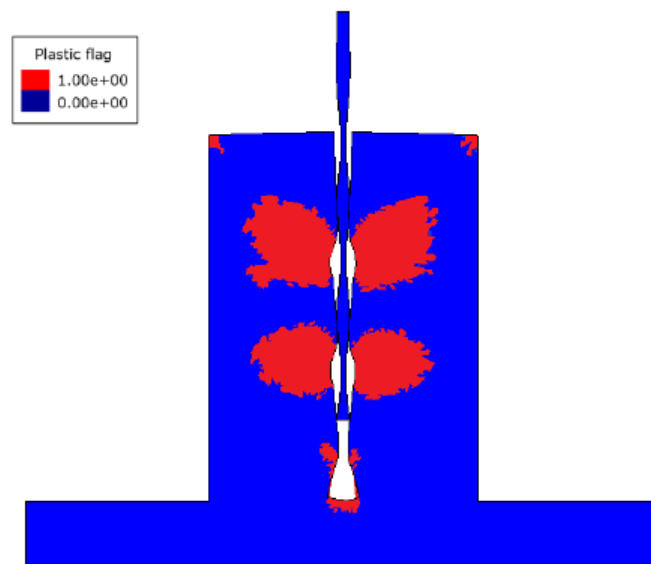


Figure 6. Plastic zone areas (in red color) detected by the numerical model at $\delta = 3$ mm.

4 Conclusions

This study developed a finite element (FE) model to investigate the pullout behavior of twisted steel fiber-reinforced concrete. A surface-based cohesive formulation coupled with damage evolution and a friction law proved effective for simulating the pullout process. The FE model demonstrated strong agreement with experimental results for the twisted steel fiber, validating the reliability and accuracy of the numerical approach. Using a mesh comprising approximately 5000 elements was found to be sufficient to accurately simulate the pullout behavior of the twisted steel fiber.

Furthermore, the contact formulation employed in the model effectively captured the mechanisms at the fiber/matrix interface, particularly concerning fiber debonding and pullout. The FE model was also capable of identifying the distribution of plastic strains and damage around the interface. The shear stress transfer mechanisms at the fiber interface were validated through experimental tests, revealing the evolution of shear stresses along the longitudinal length of the fiber.

Acknowledgements. The authors would like to thank Tecgraf Institute for all support and assistance during the execution of this project.

Authorship statement. The authors hereby confirm that they are the sole liable persons responsible for the authorship of this work, and that all material that has been herein included as part of the present paper is either the property (and authorship) of the authors, or has the permission of the owners to be included here.

References

- [1] H. Hao and Y. Hao, "Performance of spiral-shaped steel fibre reinforced concrete structure under static and dynamic loads," University of Queensland Library, Dec. 2016, pp. 58–68. doi: 10.14264/uql.2016.1186.
- [2] J. Katzer, "Steel fibers and steel fiber reinforced concrete in civil engineering," *Pacific Journal of Science and Technology*, vol. 7, pp. 53–58, 2006, [Online]. Available: <http://www.wbiis.tu.koszalin.pl/ltb/>
- [3] C. Sujivorakul, "Development of high performance fiber -reinforced cement composites using twisted polygonal steel fibers," University of Michigan, Ann Arbor, 2002.
- [4] Y. Hao and H. Hao, "Pull-out behaviour of spiral-shaped steel fibres from normal-strength concrete matrix," *Constr Build Mater*, vol. 139, pp. 34–44, May 2017, doi: 10.1016/j.conbuildmat.2017.02.040.
- [5] M. Congro, "Análise Probabilística da Capacidade de Carga de Vigas de Concreto Reforçadas com Fibras de Aço," PUC-Rio, Rio de Janeiro, 2017.
- [6] Z. Yang, B. M. Zhang, L. Zhao, and X. Y. Sun, "Stress transfer around a broken fiber in unidirectional fiber-reinforced composites considering matrix damage evolution and interface slipping," *Sci China Phys Mech Astron*, vol. 54, no. 2, pp. 296–302, Feb. 2011, doi: 10.1007/s11433-010-4148-1.
- [7] Y.-S. Tai and S. El-Tawil, "Computational investigation of twisted fiber pullout from ultra-high performance concrete," *Constr Build Mater*, vol. 222, pp. 229–242, Oct. 2019, doi: 10.1016/j.conbuildmat.2019.06.146.
- [8] Yu. N. Rabotnov, F. A. Leckie, and W. Prager, "Creep Problems in Structural Members," *J Appl Mech*, vol. 37, no. 1, pp. 249–249, Mar. 1970, doi: 10.1115/1.3408479.
- [9] J. Lubliner, J. Oliver, S. Oller, and E. Oñate, "A plastic-damage model for concrete," *Int J Solids Struct*, vol. 25, no. 3, pp. 299–326, 1989, doi: 10.1016/0020-7683(89)90050-4.
- [10] P. Rossi, P. Acker, and Y. Malier, "Effect of steel fibres at two different stages: The material and the structure," *Mater Struct*, vol. 20, no. 6, pp. 436–439, Nov. 1987, doi: 10.1007/BF02472494.
- [11] J. Lubliner, J. Oliver, S. Oller, and E. Oñate, "A plastic-damage model for concrete," *Int J Solids Struct*, vol. 25, no. 3, pp. 299–326, 1989, doi: 10.1016/0020-7683(89)90050-4.